

# HST-FOS Observations of M87: Ly $\alpha$ Emission from the Active Galactic Nucleus<sup>1</sup>

Ravi Sankrit<sup>2</sup>, Kenneth R. Sembach<sup>2</sup>, Claude R. Canizares<sup>3</sup>

## ABSTRACT

The Faint Object Spectrograph on the Hubble Space Telescope was used to obtain spectra of the central region of M87. These spectra cover the wavelength range 1140 Å – 1606 Å and have a resolution of  $\sim 1$  Å. The nuclear continuum is clearly visible in the spectra. The only strong line that is observed is Ly $\alpha$ , which has a velocity width of about 3000 km s<sup>-1</sup> (higher than the width of any line previously observed in the M87 nucleus). There is also a marginal detection of C IV  $\lambda$ 1549. The ratio of Ly $\alpha$  to C IV in the nuclear spectrum is at least a factor of 2 higher than in a spectrum taken at a position on the disk  $\sim 0''.6$  away from the nucleus by Dopita et al. This enhancement of Ly $\alpha$  at the nucleus could point to significant differences in the properties of the emitting gas and/or the excitation mechanism between the outer and inner disk regions. The strength of the observed Ly $\alpha$  places limits on the properties of the absorbing gas present within M87. For instance, if the hydrogen column at the systemic velocity of M87 is greater than about 10<sup>18</sup> cm<sup>-2</sup> then it can cover only a small fraction of the line emitting region. Spectra separated by 5 days show a 60% difference in the Ly $\alpha$  flux, but the same continuum level. This could be due to either a displacement between the aperture positions for the two sets of observations, or it could be due to intrinsic variability of the source. The current observations do not strongly favor either of these alternatives. The observations do show, however, that the Ly $\alpha$  line is a useful tracer of kinematics in the M87 nucleus.

*Subject headings:* galaxies: active — galaxies: individual(M87) — galaxies: nuclei

---

<sup>1</sup>Based on observations with the NASA/ESA *Hubble Space Telescope*, obtained at the Space Telescope Science Institute, which is operated by AURA, Inc., under NASA contract 5-26555.

<sup>2</sup>Department of Physics and Astronomy, 3400 N. Charles St. The Johns Hopkins University, Baltimore, MD 21218

<sup>3</sup>Center for Space Research, MIT, Cambridge, MA 02139

## 1. Introduction

The giant elliptical galaxy M87 (NGC 4486), at the center of the Virgo cluster with its spectacular jet, is a prototypical active galactic nucleus. Its nucleus contains a luminous accretion disk, discovered in a *Hubble Space Telescope* (HST) WFPC2 H $\alpha$  image (Ford et al. 1994). Spectroscopy of the region using the HST *Faint Object Spectrograph* (FOS) showed that the gas in the disk is in Keplerian rotation about a mass concentration of  $\sim 2.5 \times 10^9 M_{\odot}$  within the inner  $0''.25$  of the nucleus (Harms et al. 1994, henceforth H94). These two companion papers provided strong evidence for the existence of a supermassive black hole at the center of M87, something first suggested several years ago (Young et al. 1978, Sargent et al. 1978). Subsequent investigations of the disk kinematics have strengthened the case for such a black hole (Marconi et al. 1997, Macchetto et al. 1997).

More recently, based on the variability of the nuclear continuum, the continuum spectral shape, strong relativistic boosting, and the detection of superluminal motions in the jet, it has been suggested that M87 could be a misaligned BL Lac object (Tsvetanov et al. 1998a). FOS observations of the disk away from the nucleus show a LINER spectrum with evidence for shock heated gas (Dopita et al. 1997, henceforth D97). The luminosity of the M87 nucleus at all wavelengths is significantly lower than the luminosity of typical radio loud quasars such as 3C 273, which led Reynolds et al. 1996 to suggest that the M87 black hole accretes in an advection-dominated mode. Properties of the M87 nucleus and disk have been reviewed recently by Ford & Tsvetanov 1998, Tsvetanov et al. 1998b and Tsvetanov et al. 1998c.

In this paper we present new FOS observations of the M87 nucleus. These spectra differ from earlier spectra of M87 taken with the same instrument – they are centered on the nucleus, they have higher spectral resolution, and they cover the ultraviolet wavelength range. In the following section we describe the observations.

## 2. Observations

The observations presented in this paper were taken as part of HST program GO-5921 (P.I. Canizares). Spectra of the M87 nucleus (R. A.  $12^h30^m49^s.43$ , Dec.  $+12^{\circ}23'27''.9$  J2000) were taken through the  $0''.26$  diameter circular aperture, using the G130H grating, which covers the wavelength region  $1140 \text{ \AA} - 1606 \text{ \AA}$ . The spectra have a resolution of about  $1 \text{ \AA}$ , corresponding to  $\sim 250 \text{ km s}^{-1}$  at the rest wavelength of the Ly $\alpha$  line ( $1215.7 \text{ \AA}$ ). The data were reduced with the standard HST pipeline software available at the time of the observations. Inspection of the zero-levels of the spectra near the Ly $\alpha$  line showed that

there are no systematic background errors in the reduced data.

An initial set of observations obtained in May 1996 had a pointing error – the aperture was centered more than  $1''$  away from the nucleus. A second set of observations was obtained in January 1997 with the correct pointing. Five spectra having a total exposure time of 9970 seconds were taken on January 18, and six spectra having a total exposure time of 12,720 seconds were taken on January 23. In the following discussion, unless explicitly mentioned otherwise, we will be referring to the summed spectrum from the second set of observations. When needed, we will refer to the May 1996 observations as “epoch 1”, and distinguish between the January 18 and January 23, 1997 observations by referring to them as “epoch 2a” and “epoch 2b”, respectively. The observations are preserved in the HST archive with identifications Y3170104T–9T (epoch 1), Y3175106T–AT (epoch 2a), and Y3175202T–7T (epoch 2b).

In the following sections we present our results. Continuum emission from the nucleus is detected at levels consistent with previous observations.  $\text{Ly}\alpha$  is the only emission line that is clearly detected, though there is a marginal detection of  $\text{C IV } \lambda 1549$ . The  $\text{Ly}\alpha$  flux in the epoch 2b spectrum is significantly higher than in the epoch 2a spectrum. The difference is due either to an offset in the aperture positions at the two epochs, which leads to sampling of slightly different regions of the nucleus, or to intrinsic temporal variability in the source on a 5 day time scale.

### 3. The Nuclear Continuum

In Figure 1 we plot the observed flux ( $\nu F_\nu$ ) against frequency between  $2.0 \times 10^{15}$  Hz and  $2.4 \times 10^{15}$  Hz ( $1500 \text{ \AA} - 1250 \text{ \AA}$ ) for both epoch 1 (dotted line) and epoch 2 (solid line). The epoch 1 observations were centered  $1''.4$  away from the nucleus, which at the distance of M87 (15 Mpc, following H94) corresponds to about 100 pc. The continuum at this location is essentially zero. The average epoch 2 value  $\nu F_\nu \approx 1.2 \times 10^{-12} \text{ erg s}^{-1} \text{ cm}^{-2}$  is the same as that presented by Tsvetanov et al. 1998b and is also consistent with the value obtained by H94 at  $7 \times 10^{14}$  Hz (see Table 1 of Reynolds et al. 1996). The wavelength range of our spectrum is too limited to derive an accurate spectral index for the emission.

### 4. Line Emission

In Figure 2 we plot the spectrum of the M87 nucleus between  $1200 \text{ \AA}$  and  $1250 \text{ \AA}$  (solid line). The  $\text{Ly}\alpha$  emission line is clearly separated from the geocoronal emission

(expectedly, since the systemic velocity of the galaxy is about  $1300 \text{ km s}^{-1}$ ; H94). The dotted and dashed lines show two estimates of the absorption due to Galactic hydrogen as a function of wavelength. (The transmitted fraction can be read off the numbers on the y-axis scale directly). The dotted curve was derived from the Galactic H I 21cm emission profile presented by Davies & Cummings 1975, which when integrated yields a total column  $N(\text{H I}) \approx 3.4 \times 10^{20} \text{ cm}^{-2}$ . Their 21cm profile shows a broad emission wing from  $\approx +20$  to  $+60 \text{ km s}^{-1}$ . We checked their result using the stray-radiation corrected Leiden/Dwingeloo survey (Hartmann & Burton 1997). We derived an emission profile in the direction of the M87 nucleus by averaging 8 spectra obtained at points surrounding the nucleus at an angular distance of  $1^\circ$ . The positive velocity wing is not present in either the individual or averaged stray-corrected spectra. We find an integrated  $N(\text{H I}) \approx (2.1 \pm 0.3) \times 10^{20} \text{ cm}^{-2}$ , or about 62% of the Davies & Cummings (1975) value. The maximum  $N(\text{H I})$  in any of the 8 spectra is  $2.6 \times 10^{20} \text{ cm}^{-2}$ . We show the corresponding absorption profile as a dashed curve in Figure 2. The exact shape of the  $\text{Ly}\alpha$  absorption is less sensitive to the details of the velocity distribution than to the total value of  $N(\text{H I})$ . One effect of the Galactic absorption is that the observations provide only a lower limit to the intrinsic  $\text{Ly}\alpha$  emissivity of the source. The apparent line centroid of the M87 emission may be skewed to slightly higher velocities because the Galactic absorption lies on the negative velocity side of the M87  $\text{Ly}\alpha$  profile.

The observed  $\text{Ly}\alpha$  emission profile is very wide, extending from  $1218 \text{ \AA}$  to  $1230 \text{ \AA}$ . This implies a total velocity width of about  $3000 \text{ km s}^{-1}$ . The peak flux occurs at  $1222 \text{ \AA}$ , which corresponds to a velocity of about  $1480 \text{ km s}^{-1}$ . This is consistent with the systemic velocity of M87 ( $1309 \text{ km s}^{-1}$ ; H94) since the spectral resolution is only  $250 \text{ km s}^{-1}$ . The observed flux, integrated between  $1218 \text{ \AA}$  and  $1230 \text{ \AA}$  is  $\sim (8.9 \pm 0.1) \times 10^{-14} \text{ erg s}^{-1} \text{ cm}^{-2}$ . If we assume that the emission fills the  $0''.26$  diameter aperture, this implies a surface brightness of  $\sim 1.7 \times 10^{-12} \text{ erg s}^{-1} \text{ cm}^{-2} \text{ arcsec}^{-2}$ .

The  $\text{Ly}\alpha$  emission profile (Figure 2) also exhibits a shape discontinuity at  $\sim 1226 \text{ \AA}$ . In order to quantify the velocity width of the profile in a more formal manner, we created an artificial line profile by reflecting the observed line profile to the longer wavelength side about the observed peak. We then fit the resulting profile with the sum of two gaussians with FWHM equal to  $1525 \text{ km s}^{-1}$  and  $3490 \text{ km s}^{-1}$ , each contributing roughly half the flux. The narrower component has a velocity width comparable to those found by H94 for the optical lines in their FOS spectrum of the nucleus. The broad component has a line width higher than has been observed in optical emission lines. We emphasize that the velocity widths depend in part on the assumption that the broad and narrow components are centered at the same wavelength and have symmetric velocity distributions about this wavelength.

We estimate the intrinsic Ly $\alpha$  intensity of the M87 nucleus by correcting the observed flux for the Galactic absorption shown in Figure 2. For absorbing column densities of  $2.1 \times 10^{20} \text{ cm}^{-2}$  and  $3.4 \times 10^{20} \text{ cm}^{-2}$ , the integrated fluxes between 1218 Å and 1230 Å are  $\sim 12.8 \times 10^{-14} \text{ erg s}^{-1} \text{ cm}^{-2}$  and  $\sim 16.2 \times 10^{-14} \text{ erg s}^{-1} \text{ cm}^{-2}$  respectively. Between 30% and 45% of the Ly $\alpha$  is absorbed by Galactic hydrogen. The location of the peak in the corrected profile is very sensitive to the absorbing column used because of the large corrections shortward of 1219 Å. For a two component fit, allowing the fit parameters to vary for both components simultaneously, the centroids are ill-constrained. If we repeat the exercise of fitting a symmetrized profile, then for the case of the lower absorbing column, the broad component contributes about one-fourth the intensity. (The broad component contributed half the flux in the fit to the observed profile).

The only other line we detect in our spectrum is the C IV 1549 Å line. In Figure 3 we plot our spectrum between 1500 Å and 1600 Å. The solid line is the data rebinned over 4 pixels (about 1 Å). The dotted line shows the unsmoothed data to give an idea of the noise level in the original spectrum. Overplotted on the data are two gaussians (dashed lines) added to a linear background, to simulate the “expected” C IV flux, which will be discussed next. Both gaussians have a FWHM of 15.0 Å ( $\sim 3000 \text{ km s}^{-1}$ ) and are centered at 1555.8 Å ( $\sim 1300 \text{ km s}^{-1}$ ).

Both Ly $\alpha$  and C IV  $\lambda 1549$  were observed by D97 in their spectrum of the disk at the center of M87. (Their aperture was placed so as to avoid the nucleus). In their spectrum the ratio of observed fluxes  $F_{1549}/F_{Ly\alpha} \approx 0.2$ . Applying this ratio to our Ly $\alpha$  measurement, we estimate a C IV  $\lambda 1549$  flux of  $1.8 \times 10^{-14} \text{ erg s}^{-1} \text{ cm}^{-2}$ . The stronger gaussian in Figure 3 is constructed to have this flux, and in spite of the large velocity width, it is clearly incompatible with the observations. Thus, the observed C IV to Ly $\alpha$  ratio is weaker in the nucleus than in the disk.

We can obtain the “expected” C IV flux in another way, using the H $\beta$  flux instead of Ly $\alpha$ . H94 observed the H $\beta$  flux from the nucleus to be about  $2.5 \times 10^{-15} \text{ erg s}^{-1} \text{ cm}^{-2}$  and in the D97 spectrum, the ratio  $F_{1549}/F_{H\beta} \approx 3.6$ . Using this ratio, we estimate a C IV  $\lambda 1549$  flux of  $9 \times 10^{-15} \text{ erg s}^{-1} \text{ cm}^{-2}$ , which is half the value derived using Ly $\alpha$ . The weaker gaussian in Figure 3 is constructed to have this flux, and it is a reasonable upper limit on the observed C IV emission. (Note that since the data are noisy, we do not attempt to find a “best fit” spectrum to the C IV line profile).

In our spectrum of the M87 nucleus, we observe  $F_{1549}/F_{Ly\alpha} \leq 0.1$  (see the discussion above and Figures 2 and 3). This is at least a factor of 2 lower than the value obtained by D97 for their disk spectrum. Furthermore, the Ly $\alpha$  emission in our spectrum (Figure 2) extends out to higher velocities (relative to line center) than previously reported for any line.

As discussed above, if we assume that the observed Ly $\alpha$  line is symmetric, it can be fit with two components each containing about half the flux. This makes the observed ratio of C IV to “narrow” Ly $\alpha$  compatible with the value obtained by D97. Therefore, one interpretation of our spectrum is that the narrower Ly $\alpha$  emission and all of the C IV emission comes from part of the disk which has a LINER spectrum like that observed by D97, and the remaining Ly $\alpha$  (the broad component) arises in a region with different characteristics (which may or may not be part of the disk). In this picture, the first component is due to a fast shock such as the one invoked by D97 to explain their spectrum. The second component could be due to slower shocks ( $v_{shock} \lesssim 100 \text{ km s}^{-1}$ ) which do not produce C IV, or it could be due to photoionization of material by the nuclear continuum.

It is worthwhile pointing out that the low value of C IV to Ly $\alpha$  does not rule out photoionization as a possible excitation mechanism for the putative second component. The M87 nucleus is underluminous compared to typical AGN (Reynolds et al. 1996) and the incident flux on any photoionized gas is correspondingly low. To address this issue, we used the M87 spectrum presented by Reynolds et al. 1996 to calculate simple slab geometry photoionization models using CLOUDY (Ferland et al. 1998). We find that the ionization parameter is  $10^{-3}$  for a cloud with density  $n_H = 10^6 \text{ cm}^{-3}$ , lying about 1 pc away from the nucleus. For this value of the ionization parameter, the model predicts  $F_{1549}/F_{Ly\alpha} \sim 0.01$ . Clearly such weak C IV emission would not be seen in our spectrum. We note that 1 pc corresponds to about  $0''.015$  at the distance of M87, and is about 1/100 the radius of the ionized disk (Ford & Tsvetanov 1998).

In order to distinguish between shock excited gas and photoionized gas more diagnostic lines need to be measured. Based on our present data, we conclude that the fast shock which produces the disk spectrum of D97 does not explain all the Ly $\alpha$  emission.

## 5. Absorbing Gas within M87

Absorption line systems for both our Galaxy and M87 have been observed by Tsvetanov et al. 1998b. Their near-ultraviolet and optical spectra contain broad ( $\sim 400 \text{ km s}^{-1}$ ) absorption lines arising in M87 from neutral and low ionization species (Na I, Mg I, Ca II, Mg II, Mn II, Fe II). They suggest a simple model of the nucleus in which the line of sight to the central point source passes through an outflow from the inclined, turbulent disk.

Higher resolution ( $\sim 10 \text{ km s}^{-1}$ ) optical absorption line observations of Na I and Ca II (Carter & Jenkins 1992; Carter, Johnstone & Fabian 1997) reveal at least two, and perhaps more, cool interstellar clouds in the nuclear region of M87. The absorption is spread over

at least two components at +990 and +1297 km s<sup>-1</sup>, each with an equivalent H I column density of  $\geq 5 \times 10^{17}$  cm<sup>-2</sup> and an internal velocity dispersion of  $< 7.5$  km s<sup>-1</sup>. They interpret these lines as coming from a population of clouds with radii of 10<sup>12</sup> cm – 10<sup>16</sup> cm, which covers only a fraction (perhaps 10%) of the nuclear region responsible for the continuum. High spatial resolution (beam width  $\approx 1''$ ) VLA observations of the H I 21 cm absorption in the core of M87 by van Gorkom et al. 1989 yield an optical depth of  $< 0.007$  and  $N(\text{H I}) < 5.1 \times 10^{19}$  cm<sup>-2</sup>. There is some debate about whether the total H I column density may in fact be larger than this value, but high-resolution observations of species other than trace ions such as Na I and Ca II will be needed to make an accurate assessment of the amount of gas present and its detailed velocity distribution. For the purposes of the discussion that follows, we will consider a range of values of  $N(\text{H I})$  for the M87 gas.

We note that our FOS data are not of sufficient spectral resolution and S/N to make meaningful determinations of the metal-line strengths in the M87 gas. For an H I column density of  $5 \times 10^{19}$  cm<sup>-2</sup> and a covering fraction of unity, even the strongest metal lines in this wavelength range (e.g., C II  $\lambda 1334.5$ , O I  $\lambda 1302.2$ ) would have apparent absorption depths of only  $\approx 10$ –25%, relative to the continuum, at this resolution. This is less than the  $1\sigma$  scatter of the noise about the mean continuum level.

It is possible, however, to qualitatively assess the effects the H I associated with the known interstellar clouds in M87 might have on the observed Ly $\alpha$  emission from the nucleus. In Figure 4 we plot our epoch 2 spectrum between 1210 Å and 1235 Å. Also plotted are the Ly $\alpha$  absorption profiles (again as transmittances) which we have modeled using the velocity structure for the absorbers seen by Carter, Johnstone & Fabian 1997. We have used hydrogen column values,  $N(\text{H I}) = 1 \times 10^{18}$  cm<sup>-2</sup> and  $5 \times 10^{19}$  cm<sup>-2</sup>. From Figure 4 it is clear that for the higher  $N(\text{H I})$  case, most of the Ly $\alpha$  emission would be suppressed due to hydrogen absorption. Perhaps equally important, photoelectric heating of dust grains present in cool absorbing gas would efficiently destroy Ly $\alpha$  photons (Spitzer 1978). Yet we detect strong Ly $\alpha$  emission with little evidence of a sharp discontinuity in the profile at the velocities of the M87 absorbers. This implies that the absorbing gas covers only a fraction of the line emitting region. More information is needed about the velocity structure and distribution of gas along the sight line to adequately model the radiative transfer of resonance line photons escaping the nuclear regions of M87.

Spectral fits to moderate resolution X-ray data from M87 with the solid state detector on the Einstein Observatory gave evidence for the presence of excess absorption, in the central parts of this very extended source (White et al. 1991). If attributed to material with cosmic abundances, the implied excess hydrogen column density was  $15 \times 10^{20}$  cm<sup>-2</sup>. By analogy to other clusters, this absorption was associated with the apparent cooling

of the X-ray emitting gas. An ASCA observation by Matsumo et al. 1996 failed to detect such large absorption but suggested the presence of an excess column density of  $\sim 2.5 \times 10^{20} \text{ cm}^{-2}$ . Both these values are clearly ruled out along the line of sight to the nucleus by our observations (Figure 4), if the hydrogen is neutral. Since hydrogen has a negligible contribution to the X-ray absorption cross section, we cannot rule out a partially ionized absorber.

## 6. Ly $\alpha$ Flux Variations

In the top panel of Figure 5 the epoch 2a spectrum (solid line) and the epoch 2b spectrum (dotted line) are plotted between 1200 Å and 1250 Å. It is clear from the plot that the Ly $\alpha$  flux is significantly higher in the later observation. The observed fluxes integrated between 1218 Å and 1230 Å (cf. §4 above) are  $6.6 \times 10^{-14} \text{ erg s}^{-1} \text{ cm}^{-2}$  and  $10.7 \times 10^{-14} \text{ erg s}^{-1} \text{ cm}^{-2}$  for epochs 2a and 2b respectively, corresponding to a 60% increase. In the bottom panel, the ratio of flux in the epoch 2b spectrum to the flux in the epoch 2a spectrum is plotted for this narrower wavelength range. The epoch 2b flux is higher over the entire line, with the ratio jumping from  $\sim 1.3$  to  $\sim 2.4$  at 1223 Å. Also shown in the figure are plots of the fluxes in arbitrary units. The plots of fluxes as well as the ratio have been binned over 4 pixels for clarity.

There are two possible explanations for the flux differences observed. First, the aperture locations for the two observations could have been offset in such a way as to cause the observed fluxes to be different. Second, the source may actually be variable on a time scale of  $\sim 5$  days. Both alternatives are interesting, though we cannot confidently distinguish between them without additional observations.

### 6.1. *Offset in Aperture Location*

The flux from the center of M87 is dominated by the nucleus. However, the existence of an extended emitting disk makes it somewhat difficult to center the 0".26 FOS aperture exactly on the nucleus. The target was acquired for the epoch 2a observations using a series of ACQ/PEAK raster scans (Voigt & Keyes 1997). For epoch 2b, the earlier epoch 2a co-ordinates were “re-acquired” and a single scan was performed to find the peak. We examined the ACQ/PEAK data and estimated that the offset in aperture positioning could be as much as 0".1 between the two epochs. However, from the actual counts in the ACQ/PEAK data, and more importantly because the continuum flux levels are the same in



both epoch 2a and epoch 2b spectra, we believe that the nucleus itself was included in the  $0''.26$  diameter aperture in both cases. This is supported by the fact that we find the same continuum flux in our spectra that Tsvetanov et al. 1998b found in their low resolution FOS spectrum of the nucleus.

The center of M87 is a very complicated region where, in addition to the black hole and Keplerian disk, there are a number of optical filaments which are thought to originate in a wind from the disk. Large non-circular velocities have also been observed at several locations within  $0''.2$  ( $\sim 14$  pc) of the nucleus. (See Ford & Tsvetanov 1998 for a review of these and other properties of the region). Therefore, an aperture displacement of  $0''.1$  between two observations could lead to a significant change in the observed Ly $\alpha$  flux. At the same time, the velocity distribution of the emitting regions must be such that it reproduces the increase in flux as a function of wavelength over the entire line (Figure 5, bottom panel). Future studies with accurate aperture (or slit) positioning will be able to use the Ly $\alpha$  line to map out the kinematics of the nuclear region. We note that the estimated positioning error of  $0''.1$  corresponds to about 7 pc at the distance of M87 (which we take to be 15 Mpc). This is  $\sim 6 \times 10^4 R_{Schwarzschild}$  (of the central black hole) and about 1/15 the radius of the ionized disk.

## 6.2. Variability

Variability is a fundamental property of active galactic nuclei (e.g., Krolik 1999) and has been observed in the optical continuum of the M87 nucleus (Tsvetanov et al. 1998a). Variability at optical wavelengths typically implies variability in the ultraviolet continuum as well. Photoionization can be an important mechanism for producing line emission. If the photoionized gas is ionization bounded, then an increase in the ionizing flux will lead to stronger Ly $\alpha$  emission. This is compatible with the M87 nucleus being quite transparent to Ly $\alpha$  photons (as we discussed in §5) if the emitting gas is concentrated in dense clouds that have a sufficiently low covering factor. Furthermore, due to the travel time of photons from the central source to the line emitting gas, the change in the continuum will be observed first and change in line emissivity will be delayed (e.g., Horne 1999). The increase in Ly $\alpha$  emission need not be related to an increase in the continuum flux. It could also be a result of some variability in the accretion flow that causes some excess gas to be excited (either by photoionization or by shocks). In any case, line emission variability in the M87 nucleus is in itself not a surprising phenomenon.

The shortest time scale for continuum variability observed by Tsvetanov et al. 1998a was about a month. In their set of 6 observations there was only one pair separated by less

than a week (the separation was 23 hours). Their sampling was not sufficient to exclude the possibility of 5 day variations. Only continued monitoring of M87 can show reliably whether variability on a 5 day time scale occurs at all, and if so how common the occurrence is.

If we have serendipitously observed intrinsic variation in the Ly $\alpha$  flux on a time scale  $\tau \sim 5$  days, then the observations set a limit on the size of the emitting region. The limiting size is  $c\tau \sim 1.3 \times 10^{16}$  cm (0.005 pc). This is equivalent to about 100  $R_{Schwarzschild}$ .

## 7. Summary

The spectrum of the M87 nucleus between 1140 Å and 1606 Å (with 250 km s<sup>-1</sup> velocity resolution) shows continuum emission consistent with previous observations and strong Ly $\alpha$  emission with a large velocity width ( $\sim 3000$  km s<sup>-1</sup>). The C IV  $\lambda 1549$  line is marginally detected. From the strength of the Ly $\alpha$  and limit on the C IV emission we infer that the nuclear line spectrum is different from the line spectrum of the Keplerian disk presented by D97. In particular the strong Ly $\alpha$  (and correspondingly, the weak C IV) could be due to the presence of photoionized gas in addition to the shocked gas invoked by D97 to explain the disk spectrum. It could also be due to slower shocks that do not produce C IV emission.

The strength of the observed Ly $\alpha$  also allows us to place some rough limits on the amount and distribution of the absorbing gas present within M87. If the hydrogen column of the gas giving rise to the observed metal lines (in absorption) is greater than about  $10^{18}$  cm<sup>-2</sup> then it cannot cover more than a small fraction of the Ly $\alpha$  emitting region.

Our observations show that the Ly $\alpha$  line can be used effectively to probe the kinematics of the central region of M87. Spectra taken 5 days apart reveal a 60% increase in the Ly $\alpha$  flux, but no change in the continuum. The Ly $\alpha$  flux difference is either due to (i) an offset in the aperture position between the two observations or (ii) intrinsic variability of the source. To distinguish between these two possibilities additional spectra with high pointing accuracy ( $\leq 0''.05$ ) and sufficiently frequent time sampling (order of days) will be needed. As pointed out by Tsvetanov et al. 1998a, such observations would have to be done with space-based telescopes since the effects from background stars and the jet make it difficult to isolate nuclear emission even in the best of seeing conditions from the ground.

The kinematics of the central region of M87 could be mapped in detail using the high spatial and spectral resolution capabilities of the *Space Telescope Imaging Spectrograph* (STIS) on board the HST. A time series of long slit observations would allow one to distinguish between the competing possibilities for the observed variation in the Ly $\alpha$

emission profiles (§6) as well as to study the metal-line abundances and distribution of gas in the nuclear region. Such emission and absorption information could potentially be of great importance for understanding the properties of material in the nuclear disk and the physical processes related to the central black hole.

We thank Zlatan Tsvetanov for several discussions and Ray Lucas for assistance with tracking down the epoch 1 pointing error. We thank the anonymous referee for useful suggestions. We also thank the STScI help desk for promptly answering questions about some details of the observations. We acknowledge using CADC, which is operated by the National Research Council, Herzberg Institute of Astrophysics, Dominion Astrophysical Observatory. RS acknowledges support from grant GO-07289.01-96A from the Space Telescope Science Institute. KRS acknowledges support from NASA Long Term Space Astrophysics grant NAG5-3485. CRC and KRS acknowledge support from NASA through STScI grant 05921-01-94A.

## REFERENCES

- Carter, D. & Jenkins, C. R. 1992, MNRAS, 257, 7P
- Carter, D., Johnstone, R. M. & Fabian, A. C. 1997, MNRAS, 285, L20
- Davies, R. D. & Cummings, E. R. 1975, MNRAS, 170, 95
- Dopita, M. A. et al. 1997, ApJ, 490, 202
- Ferland, G. J. et al. 1998, PASP, 110, 761
- Ford, H. C. et al. 1994, ApJ, 435, L27
- Ford, H. C. & Tsvetanov, Z. I. 1998, The Ringberg Workshop on M87
- Harms, R. J. et al. 1994, ApJ, 435, L35
- Hartmann, D. & Burton, W. B. 1997, Atlas of Galactic Neutral Hydrogen (Cambridge: Cambridge University Press)
- Horne, K. 1999, Quasars and Cosmology, ASP Conference Series, eds. Ferland, G. & Baldwin, J. (San Francisco: ASP)
- Krolik, J. 1999, Active Galactic Nuclei (Princeton: Princeton University Press)
- Macchetto, F. et al. 1997, ApJ, 489, 579
- Marconi, A. et al. 1997, MNRAS, 289, L21
- Matsumo, H. et al. 1996, PASJ, 48, 201
- Reynolds, C. S. et al. 1996, MNRAS, 283, L111
- Sargent, W. L. W. et al. 1978, ApJ, 221, 731
- Spitzer, L. 1978, Physical Processes in the Interstellar Medium (New York: Wiley Interscience)
- Tsvetanov, Z. I. et al. 1998a, ApJ, 493, L83
- Tsvetanov, Z. I. et al. 1998b, The Ringberg Workshop on M87
- Tsvetanov, Z. I. et al. 1998c, The Ringberg Workshop on M87
- van Gorkom, J. H. et al. 1989, AJ, 97, 708

Voigt, M & Keyes, T. 1997, Hubble Space Telescope Data Handbook, v3 (Baltimore: Space Telescope Science Institute)

White, D. A. et al. 1991, MNRAS, 252, 72

Young, P. J. et al. 1978, ApJ, 221, 721

Fig. 1.— Continuum flux between  $2.0 \times 10^{15}$  Hz and  $2.4 \times 10^{15}$  Hz ( $1500 \text{ \AA}$  to  $1250 \text{ \AA}$ ) from the nucleus of M87 (solid line) and from a position  $1''$  away from the nucleus (dotted line). The continuum flux level is consistent with previous measurements (see text).

Fig. 2.— The spectrum of the M87 nucleus (solid line) showing the strong Ly $\alpha$  emission. The line is broad and well separated from the geocoronal Ly $\alpha$ . The dotted and dashed lines show two models for the absorption due to Galactic hydrogen, plotted as transmittance fractions. They correspond to hydrogen columns of  $3.4 \times 10^{20} \text{ cm}^{-2}$  and  $2.1 \times 10^{20} \text{ cm}^{-2}$  respectively.

Fig. 3.— The spectrum of the M87 nucleus showing possible C IV  $\lambda 1549$  emission. The dotted line is the unsmoothed spectrum, and the solid line is the spectrum rebinned over 4 pixels (about  $1 \text{ \AA}$ ). The dashed lines show estimated values for the C IV flux based on previous observations of M87 (see §4 for details).

Fig. 4.— The dotted and dashed lines are two models for the absorption due to hydrogen within M87, plotted as transmittance fractions. As in Figure 2 these are overplotted on the observed M87 spectrum (solid line).

Fig. 5.— Top Panel: Spectra of the M87 nucleus taken 5 days apart (epoch 2). The integrated Ly $\alpha$  flux in the later observation is about 60% higher than in the earlier observation. The change could be due to a slight offset in the aperture locations between observations or to intrinsic variability of the source. The spectrum shown in Figures 2 and 4 is an average of these two spectra. Bottom Panel: The ratio of epoch 2b flux to epoch 2a flux for the wavelength region  $1218 \text{ \AA}$  to  $1230 \text{ \AA}$ . Also shown are the observed fluxes on an arbitrary scale. The fluxes and the ratio plot have been binned over 4 pixels. The horizontal bars represent the errors introduced due to the binning.

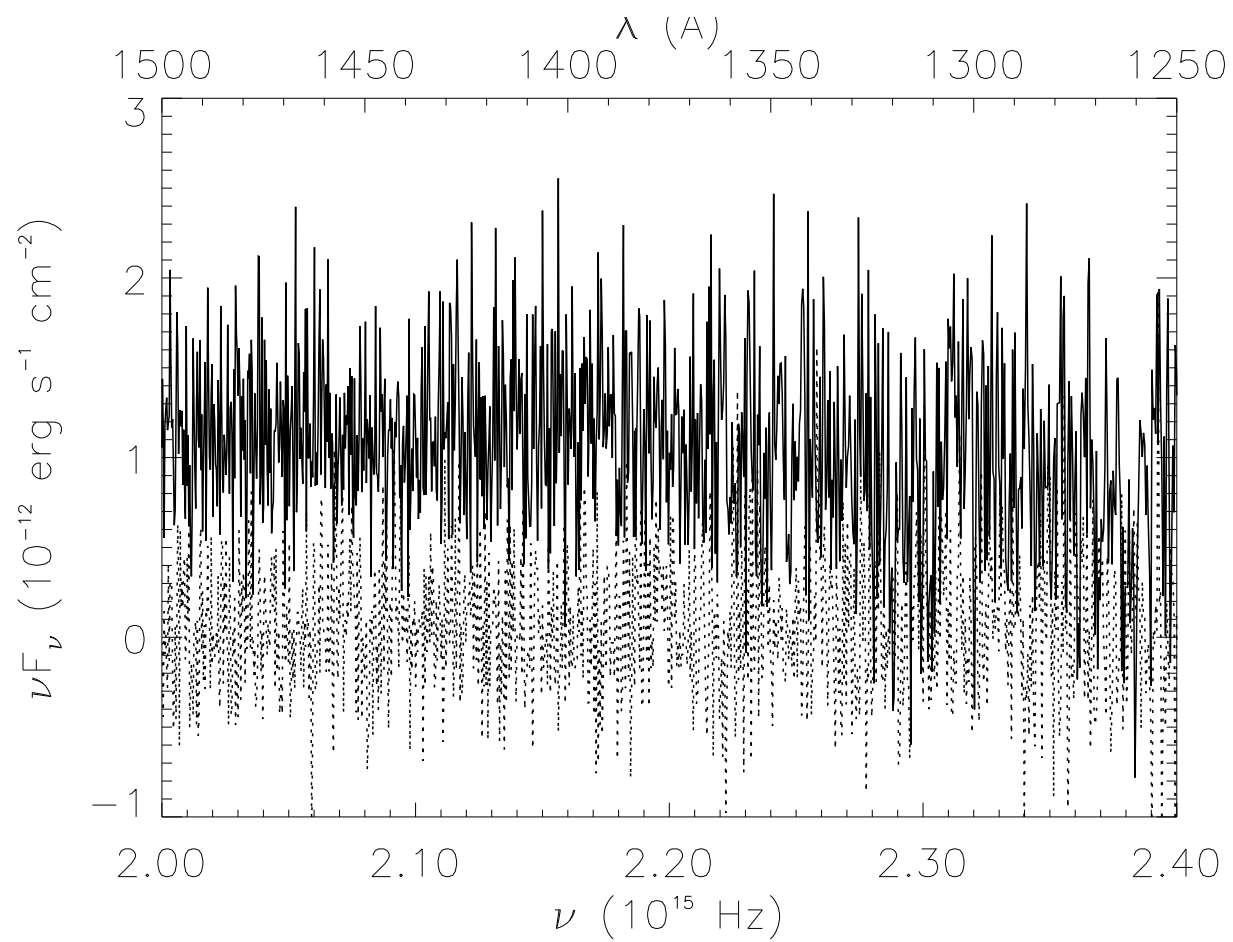


Fig. 1

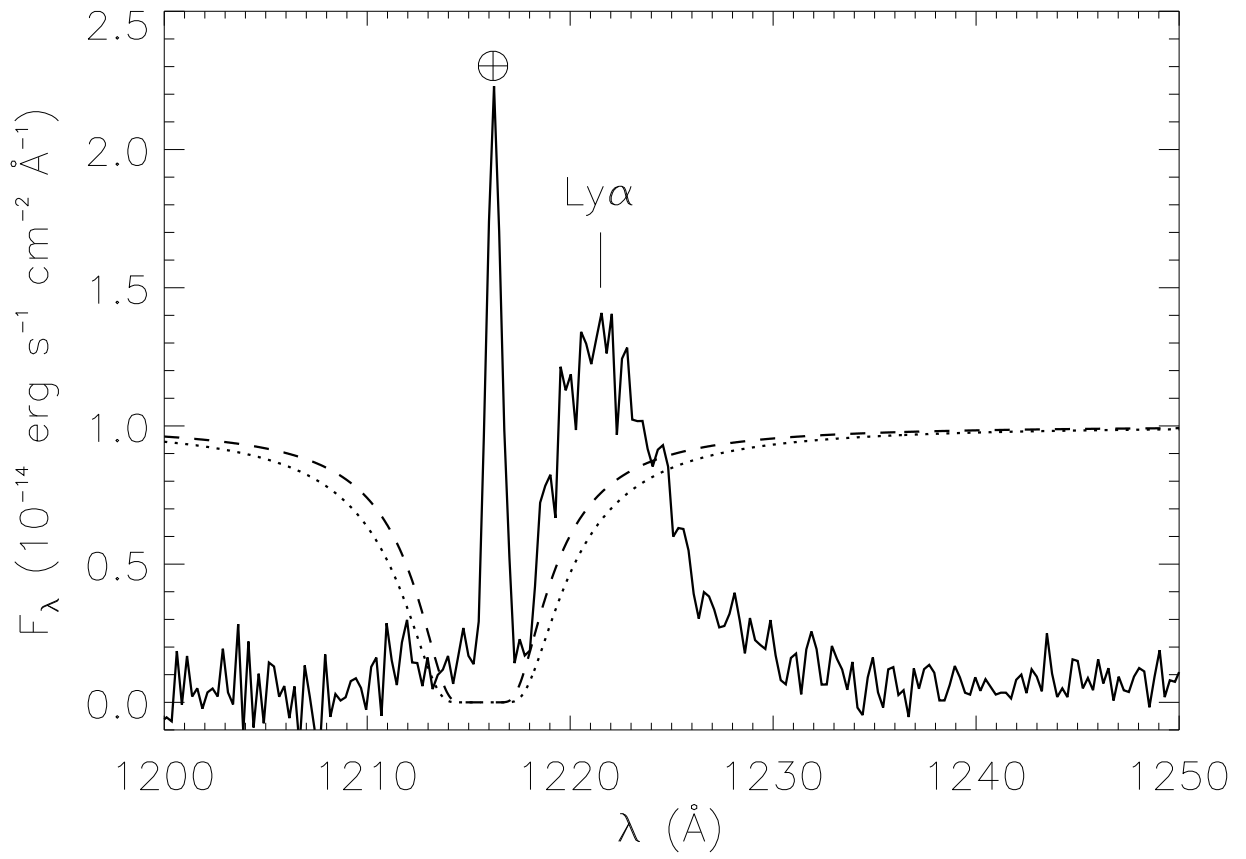


Fig. 2



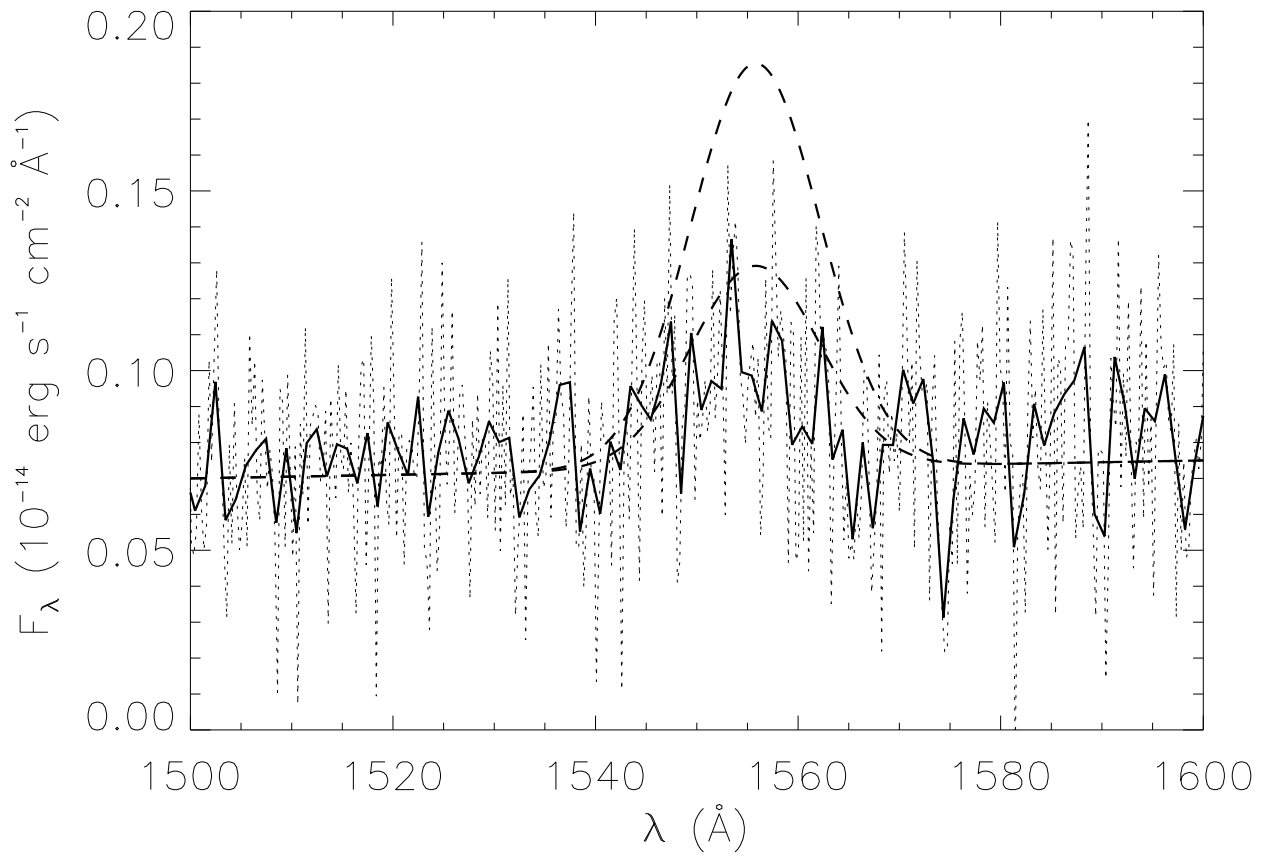


Fig. 3

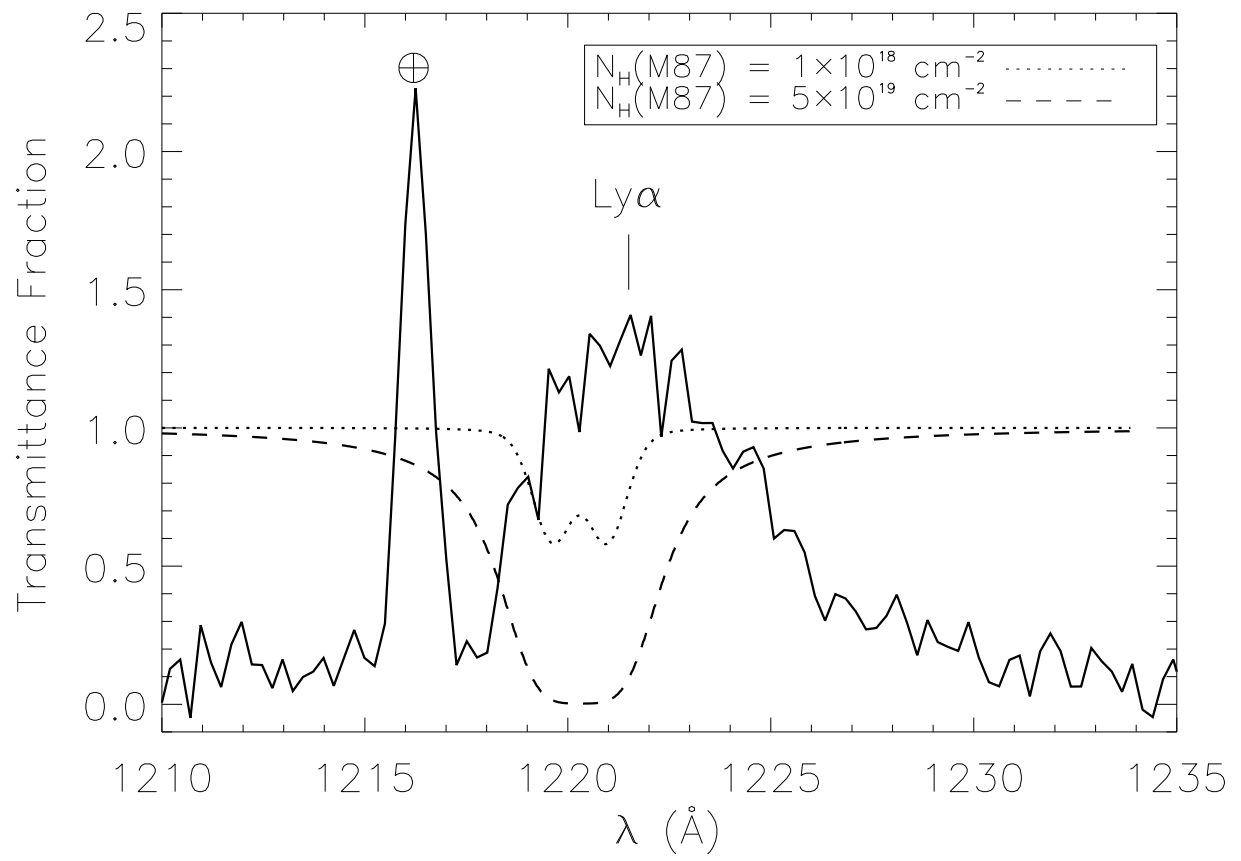


Fig. 4

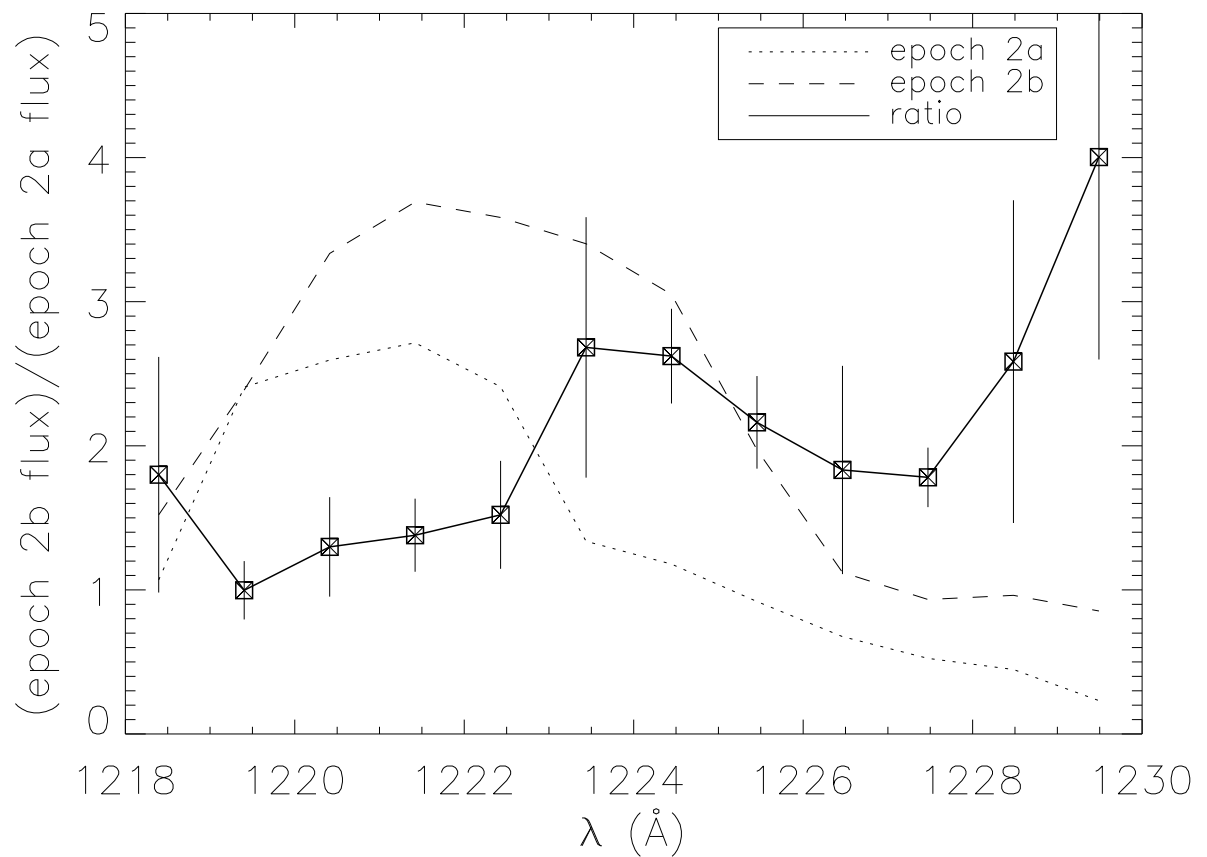
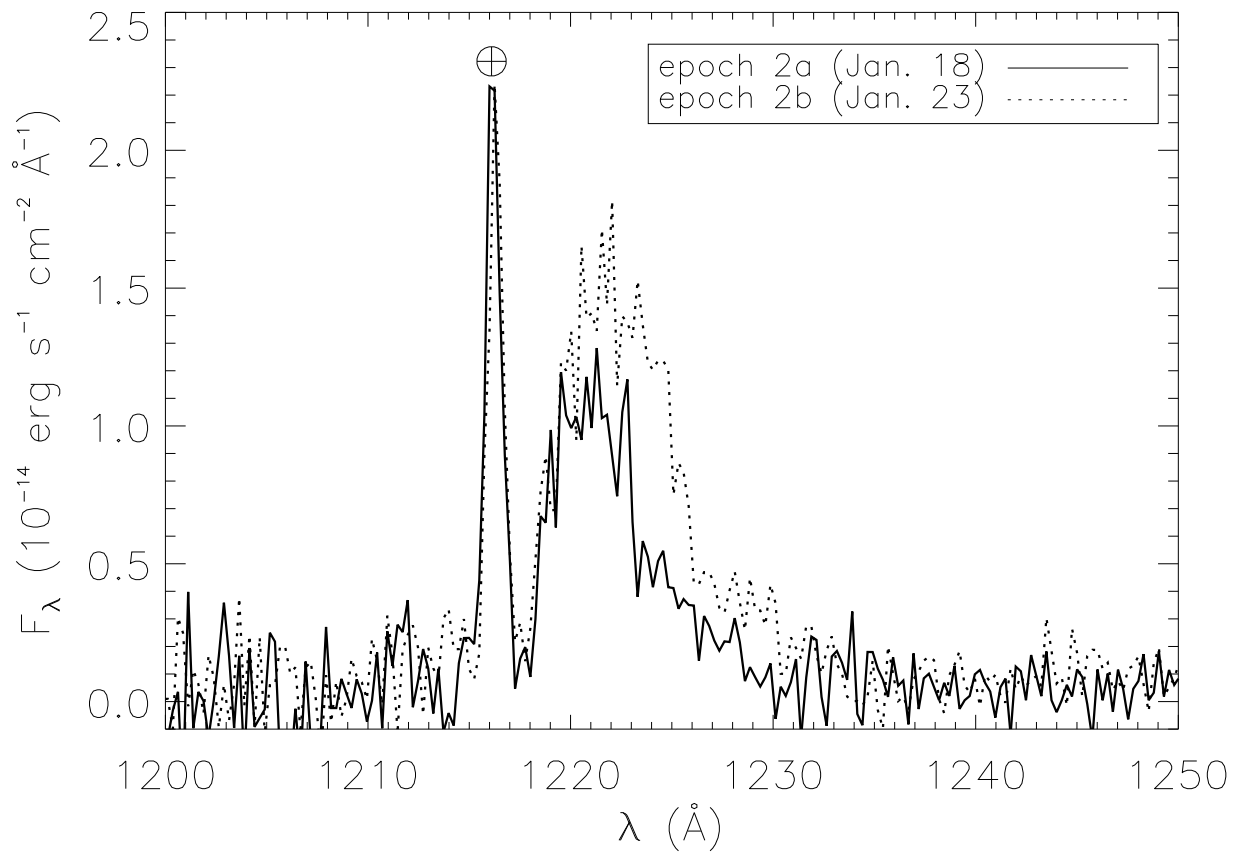


Fig. 5